World Journal of Engineering Research and Technology
WJERT
www.wjert.org
SJIF Impact Factor: 5.218

DETERMINATION OF PRESSURE DROP ACROSS A RANGE OF INLET VELOCITY IN A STAIRMAND'S HIGH EFFICIENCY CYCLONE

***Oriaku E. C., Adizue U. L., Odenigbo J. O. and Ibeagha D. C.**

Department of Engineering Research Development and Production, Projects Development Institute (PRODA) Enugu.

Article Received on 28/04/2019 **Article Revised on 18/05/2019** **Article Accepted on 09/06/2019**

***Corresponding Author**
Oriaku E. C.
Department of Engineering Research Development and Production, Projects Development Institute (PRODA) Enugu.

ABSTRACT

The need to remove suspended dust from a gas stream has led to the development of several dust collection equipment operating on different principles in use in the industry today. Cyclone is a typical example of centrifugal dust collector. Since the discovery of cyclone about a century ago, a trend of consistent research work has characterized the progressive development of Cyclone separator. These research works has a common objective of providing optimum cyclones suited for specific purposes and which offer the most favorable collection efficiency at minimum cost. Pressure drop affects cost and cyclone collection efficiency. Several attempts has been made to calculate pressure drop from fundamentals but none of them has been very satisfying and hence practical measurement is adopted in this work to more accurately determine this parameter in the Stairrmand cyclone. Pitot static tubes were used to take reading at different points on experimental rig at both No-load and load basis as shown in Figure 1. The rig was run at ten (10) different entry velocities in each case and the pressure drop determined. The results show that both percentage fine particle collection and Entry velocities increases with increase in Pressure drop. Also optimum fine particle collection (Above 88%) can be achieved at a range of 22.64 to 54.8 N/m2 and 682.2 to 1158 x 60 m/min of pressure drops and Entry velocities respectively.

KEYWORDS: Cyclone, inlet-velocity, pressure drop, cost, collection efficiency.

I. INTRODUCTION

The pressure drop across a cyclone is an important parameter for the operation of the equipment. Increased pressure drop means greater costs for power to move exhaust gas through the control device. With cyclones, an increase in pressure drop usually means that there will be an improvement in collection efficiency. One method for estimating pressure drop is based on the velocity head and the inlet and outlet dimensions of the cyclone. An alternate method bases the pressure drop on the velocity head, but includes all other effects in a single constant usually denoted by Kp (EPA, 2011). The geometrical shape of the cyclone is simple, but the pattern of air flow in the vortex is extremely complex, and theoretical calculations of the pressure drop or dust separation efficiency are correspondingly difficult. Recent experiments with cyclones have investigated the influence of factors such as cyclone diameter, showing an inverse relationship to collection efficiency (Faulkner *et al.,* 2007) and no change in cut-point, but an increase in the slope of the fractional efficiency curve with increasing cyclone size (Faulkner *et al.,* 2008). Experiments with cyclones in series showed a decreasing efficiency (expected due to the decrease in load and particle size) but also a decrease in cut-point, even though successive cyclones had the same dimensions and operating parameters (Whitelock and Buser, 2007), confirming some semi-empirical model predictions as demonstrated with very small diameter cyclones earlier (Ray *et al.,* 2000). Another experiment used a strobe light for visualization and high-time-resolution pressure measurements to quantify vortex end attachment and progression. The vortex core rotated at about the same rate as the gas in the cyclone (Peng *et al.,* 2005). Laser Doppler techniques were used to visualize swirl pattern in the cyclone and dust hopper (Hu *et al.,* 2005), (Peng *et al.,* 2002), and to look at dust agglomeration (Obermair *et al.,* 2005), especially in the dust hopper, as agglomeration is a significant factor in cyclone efficiency.

The relative dimensions of the major elements of a cyclone have long been the focus of research. However, small details can have just as large an influence on performance. For example, increasing the diameter of the cone bottom outlet has been shown to decrease pressure drop (Xiang *et al.,* 2001) and increase mass efficiency (Baker and Hughs, 1999). Other changes to the dust outlet can have significant impact on collection efficiency, such as including expansion chambers (Baker *et al.,* 1997; Holt *et al.,* 1999; Obermair and Staudinger, 2001).

The latter also documented the impact of a 2.5 cm (1 in) linear fight attached to the cone wall, running top to bottom on one side. Not only did pressure drop decrease, but recirculation of collected particles – especially fibers – was eliminated. For a constant area, the shape of the inlet is important as well.

Collection efficiency increases as the inlet becomes shorter and wider (Baker and Hughs, 1998), but only to the point that the inlet width aligns with the gas outlet tube, or vortex finder (Funk et al., 2001). Cyclone performance models have been helpful for designing „typical" dust collection systems, and for predicting trends in new design directions. But there will always be a need for lab and field testing to confirm performance. Models have two major limitations. First, they can only explain modelled variables. Dust cyclones are complex and their performance is influenced in statistically significant ways by a large number of parameters, the majority being omitted for simplicity or overlooked out of ignorance. It has long been recognized that particulate loading attenuates swirl and turbulence, reducing pressure loss and increasing efficiency at levels up to about 500 gm-3, then having the opposite impact at higher levels (Cortés and Gil, 2007), but semi-empirical (and most Computational Fluid Dynamics [CFD]) models cannot account for this phenomenon. Other examples of parameters known to influence performance that are not included in most models include things like dust outlet geometry; (Holt at al., 1999; Obermair and Staudinger, 2001); or vortex finder shape (Baker and Hughs, 1998; Lim, et al., 2004; Ogawa and Arakawa, 2006), even though they impact pressure drop and collection efficiency. In addition, models are only accurate over a limited dimensional range.

1.2 Pressure Drop: Pressure drop provides the driving force that generates gas velocity and centrifugal force within the cyclone. Several attempts have been made to calculate pressure drop from fundamentals but none of them has been very satisfying. Most correlations are based on the number of inlet velocity heads as given by the equation (Schnelle and Brown, 2002).

$$\Delta P = \frac{1}{2g_c}\rho_g V_i^2 N_H \qquad (1)$$

Where ΔP = pressure drop (N/m^2)

ρ_g = gas density (kg/m^2)

V_i = inlet velocity (m/s)

N_H = pressure drop expressed as number of the inlet velocity heads.

One of the correlations for numbers of inlet velocity heads is given by equation 2 (Schnelle and Brown, 2002);

$NH = K\Delta pi\ (D/Dc)2$ (2)

Where;

$K\Delta pi$ = constant based on the cyclone configuration and operating conditions

D = diameter of the cyclone body (mm) Dc = Dexit = diameter of exit tube (mm)

Typical value for $K\Delta pi$ in Miller and Lissman correlation is 3.2 for the standard cyclone configuration described above. Another correlation for number of inlet heads is that of Shepherd and Lapple (1940)

$NH = K\Delta p2\ Hw/D\ 2$ (3)

Where;

$K\Delta p2$ = constant for cyclone configuration and operating conditions

H = height of the inlet opening (mm) W = width of the inlet opening (mm)

De = Dexit = diameter of exit tube (mm)

The value for $K\Delta p$ in the Shepherd and Lapple correlation is different, typically ranging from 12 to 18. The Shepherd and Lapple correlation results in 8 inlet velocity heads for the standard cyclone dimensions, 6.4 inlet velocity heads for Stairmand cyclone design and 9.24 inlet velocity heads for the Swift cyclone design. As can be seen, there is substantial difference among the correlations. Again, it is best to rely on vendors experience when one‟s own experience is lacking; however, to enforce a performance guarantee, ensure that the specifications are well written and can be documented for expected conditions.

1.3 OBJECTIVES OF RESEARCH

The specific objectives of this paper are to accurately determine the pressure drop across range of inlet velocity and their relationship with percentage fine particle collection in a Stairmand‟s high Efficiency Cyclone, with view of establishing trends.

II. MATERIALS AND METHODS

The study involved the design, fabrication and characterization of an integrated dust generation and handling equipment comprising: micro-mill, cyclone, and a line of filters. Soya bean samples used for the study were “Mangu” species from Jos, Plateau State Nigeria. Performance evaluation of the system was based on varying inlet velocity and determining

pressure drop on No-load basis and Load basis (Micronized soya bean), using appropriate methods and tools.

2.1 Design and Construction of the Test Rig

The test rig for this research work was constructed and assembled at the Engineering workshop of Scientific Equipment Development Institute (SEDI) Akwuke Enugu. The Machine Design, Research and Building Department supervised the construction and assembly.

The test rig had the following features

i. Size reduction equipment (micro-mill) which crushes grains to micron size and sends the dust to the cyclone through a suction blower.

ii. A cyclone dust collector which separates the dust particles from the air iii. A line of filters connected to the vortex finder of the cyclone.

iv. Connectors which link the micro-mill to the cyclone and cyclone to the line of filters v. Measuring equipment, mainly Pitot tubes connected to the U-tube manometers See figure 1 and 11 at Appendix for the Test rig Assembly and Pitot tubes connected to the U-tube manometer.

III. RESULTS AND DISCUSSIONS

3.1 Velocity and Pressure Drop Distribution in the Cyclone on No-Load Basis.

The test rig was run at speeds ranging from 1500 rpm to 3750 rpm on no-load basis and velocity distribution across the system was recorded and the results were tabulated and shown in Appendix I. The pressure drop across the cyclone at no load basis was also determined by subtracting exit pressure from entry pressure. The result is given in Table 1. Graphs were plotted for varying parameters using MICROSOFT EXCEL 2007 and STATISTICA 7 software programmes. See explanation of abbreviations used in this work;

Entry = Inlet of the Cyclone (0.075 m from top of cyclone) BCS = Beginning of Cylindrical Section (0.16 m from top of cyclone) CCS = Centre of Cylindrical Section (0.225 m from top of cyclone) ECS = End of Cylindrical Section (0.4 m from top of cyclone) BCNS = Beginning of Conical Section (0.55 m from top of cyclone) CNS2 = Point 230 mm from beginning of Conical Section (0.68 m from top of cyclone) CNS3 = Point 330 mm from beginning of Conical Section (0.78 m from top of cyclone) CNS4 = Point 430 mm from

beginning of Conical Section (0.88 m from top of cyclone) ECNS =End of Conical Section (1.1 m from top of cyclone) TS = Terminal Section (1.275 m from top of cyclone)
VF = Vortex Finder (0.075 m above the top of cyclone)

Table 1: Determination of Pressure Drop across the Cyclone at No Load Basis.

S/n0	Rpm	Entry		Exit		Entry pressure ($p_a + \rho g \bar{o} h$), N/m^2	Exit pressure ($p_a + \rho g \bar{o} h$), N/m^2	Pressure drop P_{entry}-P_{exit} (N/m^2)
		V(m/s)	Δh(m)	V(m/s)	Δh(m)			
1	1500	12.23	5.60	6.27	2.30	101385.14	101349.40	35.44
2	1750	13.45	6.44	7.05	2.65	101394.17	101353.46	40.71
3	2000	15.72	8.18	8.63	3.43	101412.85	101361.83	51.01
4	2250	17.92	10.07	10.86	4.71	101433.15	101375.59	57.56
5	2500	19.93	11.97	12.56	5.82	101453.56	101387.51	66.05
6	2750	22.92	15.09	13.50	6.48	101487.07	101394.60	92.47
7	3000	23.08	15.27	14.02	6.86	101489.00	101395.68	93.32
8	3250	25.05	17.53	15.28	7.83	101513.27	101409.09	104.18
9	3500	27.32	20.34	16.93	9.20	101543.45	101423.81	119.64
10	3750	28.95	22.48	22.97	10.54	101566.44	101426.89	139.55

Table 2: Determination of Pressure Drop On Load Basis.

S/No	Rpm	Entry		Exit		Entry pressure ($p_a + \rho g \bar{o} h$), n/m^2	Exit pressure ($p_a + \rho g \bar{o} h$), n/m^2	Pressure drop P_{entry}-P_{exit} (n/m^2)
		V(m/s)	Δh(m)	V(m/s)	Δh(m)			
1	1500	9.15	3.72	3.43	1.13	101369.32	101338.46	30.86
2	1750	10.22	4.32	6.73	2.51	101376.47	101354.90	21.57
3	2000	11.37	5.03	8.04	3.13	101384.93	101362.29	22.64
4	2250	14.26	7.04	9.72	4.03	101408.87	101373.01	35.86
5	2500	17.14	9.38	10.98	4.78	101436.75	101381.95	54.80
6	2750	19.08	11.15	12.68	5.90	101457.84	101395.29	62.55
7	3000	18.79	10.87	13.86	6.74	101454.51	101405.30	49.20
8	3250	19.30	11.36	15.74	8.20	101460.34	101422.69	37.65
9	3500	21.72	13.79	16.45	8.79	101489.29	101429.72	59.57
10	3750	24.08	16.40	16.94	9.21	101520.39	101434.73	85.66

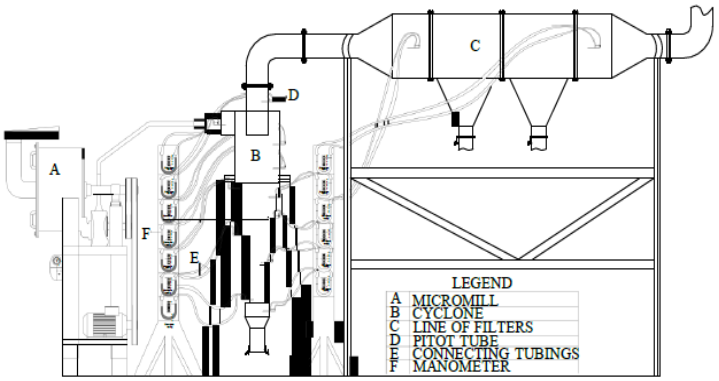

Figure 1: Schematic representation of Assembled system Source: Oriaku E. C, 2014.

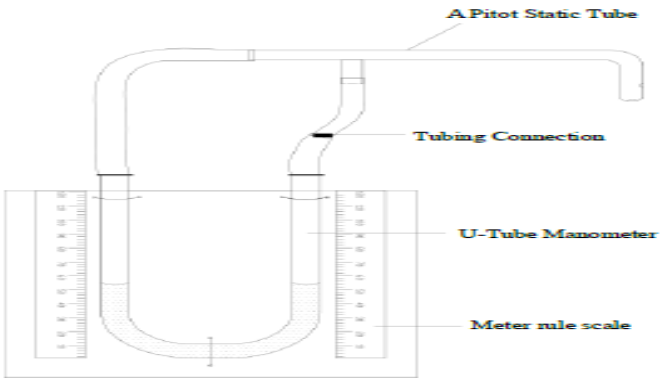

Figure 11: A Pitot Static tube Connected to U-tube Manometer.

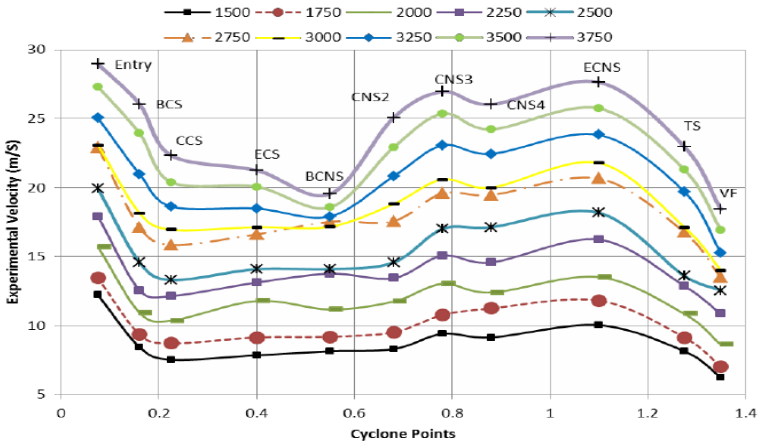

Figure 2: Combined plot showing velocity profile along the cyclone from 1500rpm to 3750 rpm.

The air entering the cyclone spins downwards due to effect of gravity and tangential component of velocity which acts downwards. From Figure 2, it can be seen that the velocity profile of speeds 1500 to 2500 rpm followed similar trend where the initial decreases in velocities from entry continued to the center of cylindrical section. These velocities then increased until the end of conical section, after which they all dropped at the terminal section. These increases in velocity are expected to influence particle collection at the terminal section. The speeds of 2750 to 3750 rpm also had similar trend. With the exception of 2750 and 3000rpm speeds the velocities at entry decreased until the beginning of the conical section. A closer look at the plot shows that the velocities appeared to converge at point BCNS. The values obtained for these speeds at that point ranged from 17.17 to 19.58 m/s. The total velocity difference across all the observed speeds ranged from 5.96 to 10.52 m/s. The relationships that best described the velocity profiles in the designed cyclone were third order polynomials with their attendant equations and R2 values recorded in Table 3.

Table 3: Polynomial equations and R2 values for velocity profiles at no-load basis.

Speed (rpm)	Equation	R^2 values
1500	$Y = -28.05x^3 + 60.28x^2 - 35.69x + 13.64$	0.847
1750	$Y = -33.24x^3 + 70.15x^2 - 40.14x + 15.19$	0.884
2000	$Y = -31.14x^3 + 65.07x^2 - 37.10x + 16.82$	0.761
2250	$Y = -34.91x^3 + 73.16x^2 - 41.33x + 19.14$	0.749
2500	$Y = -44.62x^3 + 94.51x^2 - 53.95x + 22.23$	0.849
2750	$Y = -47.63x^3 + 99.50x^2 - 56.14x + 25.19$	0.866
3000	$Y = -49.61x^3 + 103.3x^2 - 57.97x + 26.00$	0.922
3250	$Y = -57.95x^3 + 121.5x^2 - 68.55x + 29.23$	0.949
3500	$Y = -63.53x^3 + 134.4x^2 - 77.06x + 32.47$	0.919
3750	$Y = -67.04x^3 + 142.2x^2 - 81.78x + 34.78$	0.905

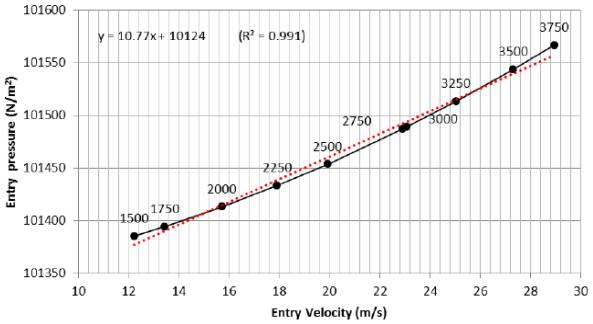

Figure 3: Entry Pressure versus Entry Velocity at no load basis.

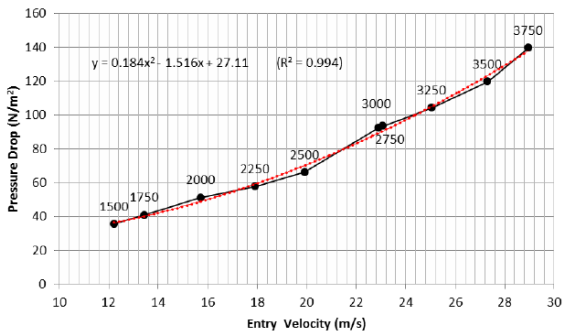

Figure 4: Pressure drop versus Velocity at no load basis.

Figure 3 shows the linear nature of the graph between entry velocity and entry pressure. This implies that entry pressure is dependent on entry velocity. The polynomial trend of the plot shows the velocity and pressure variation along the cyclone as shown in figure 4.

3.2 Velocity Distribution/ Pressure Drop on Load Basis

The velocity distribution along the cyclone was also determined on load basis as shown in Table 2 (See Appendix) and the plots are shown in Figure 5. The relationships describing

velocity along the cyclone were all trinomial with their equations stated below each plot. Pressure drop along the cyclone also followed similar trend as shown in Figure 6 and their equations shown in Table 4.

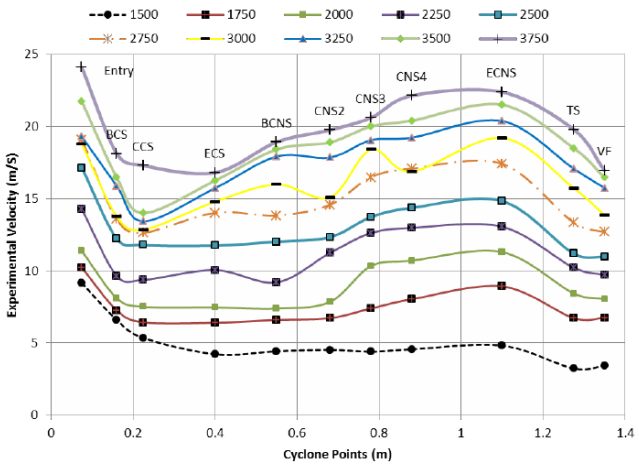

Figure 5: Combined plot of velocity distribution for the selected speeds (load basis).

Table 4: Polynomial equations and R2 values for velocity profiles at load basis.

Speed (rpm)	Equation	R^2 values
1500	$Y=-17.43x^3 + 41.02x^2 - 29.27x + 10.59$	0.942
1750	$Y = -22.33x^3 + 49.81x^2 - 30.46x + 11.58$	0.838
2000	$Y = -32.06x^3 + 68.94x^2 - 39.03x + 13.40$	0.870
2250	$Y= -34.02x^3 + 71.9x^2 - 40.03x + 15.71$	0.794
2500	$Y = -34.54x^3 + 74.13x^2 - 43.52x + 18.82$	0.822
2750	$Y = -40.51x^3 + 84.96x^2 - 47.41x + 20.67$	0.789
3000	$Y = -36.53x^3 + 75.40x^2 - 39.76x + 19.82$	0.700
3250	$Y = -34.28x^3 + 69.25x^2 - 34.68x + 20.23$	0.768
3500	$Y = -42.99x^3 + 89.19x^2 - 47.15x + 22.95$	0.764
3750	$Y = -48.30x^3 + 102.6x^2 - 57.63x + 26.41$	0.880

From the combined graphs in Figure 5, it is observed that there was decrease in velocity from inlet to end of cylindrical section for speeds below 2500 rpm and speed of 3750 rpm with the exception of 2250rpm which had a slight increase at the centre of the cylindrical section. For speeds above 2500 rpm, the decrease in velocity terminated at the centre of the cylindrical section with attendant increases beginning at the same point. It was also observed that for all speeds there was increase in velocity in the conical section of the cyclone and decrease in the terminal sections and vortex finder. Speeds of 1500, 1750 and 2500 rpm gave the smoothest transitions between sections of the cyclone and hence better velocity profiles. The above trend was also observed for pressure drop along the cyclone as shown in the Figure 6 below.

This similarity shows that pressure is dependent on velocity along the cyclone.

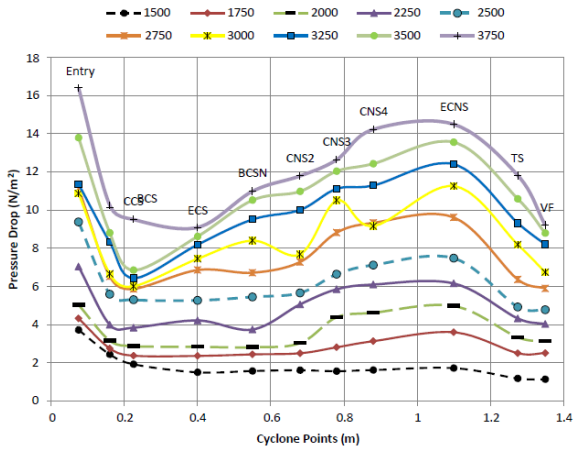

Figure 6: Combined plot of Pressure drop for the selected speeds (load basis).

The figure 7 below shows that a linear relationship exists between entry pressure and entry velocity as speeds increased from 1500rpm to 3750rpm. Speeds of 2750, 3000 and 3250 showed very little increase. This differed from what was obtained in Figure 8 where the pressure drop at these speeds occurred at almost the same velocity reading. The plots are similar to that reported by Faulkner and Shaw (2005) for 1D3D and 2D3D cyclones. They did differ in their best fit models as 1D3D and 2D3D cyclones gave an exponential mathematical model while this gave a polynomial model. It can therefore be inferred that the peak performance of the designed system should occur within this speed range.

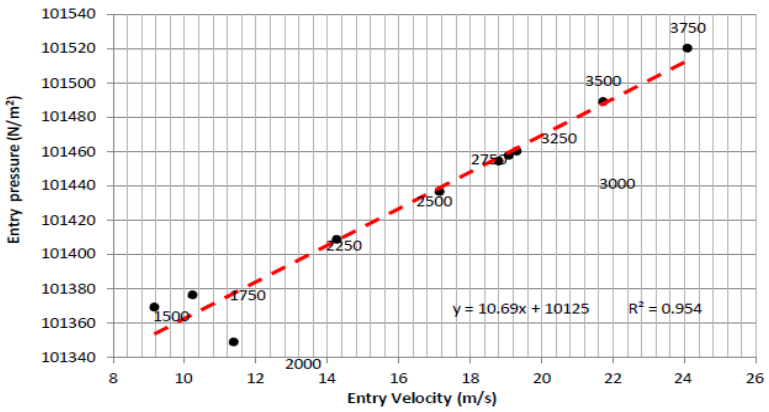

Figure 7: Entry Pressure versus Entry Velocity on load basis.

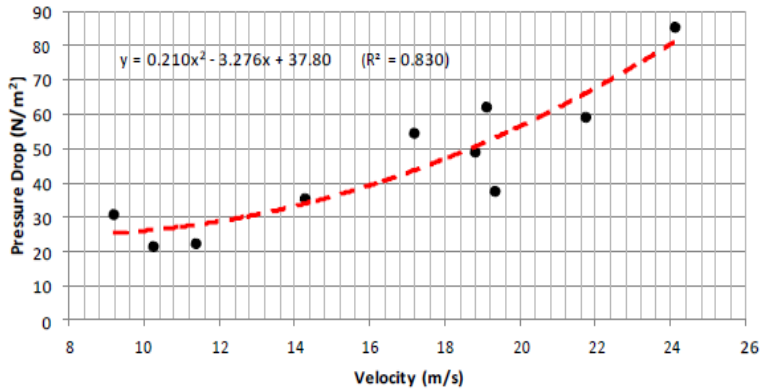

Figure 8: Pressure drop versus Velocity on load basis.

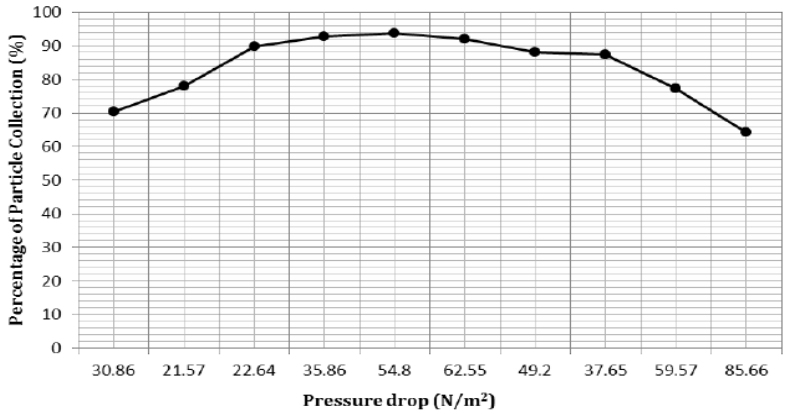

Figure 9: Pressure drop versus Percentage of Particle Collection.

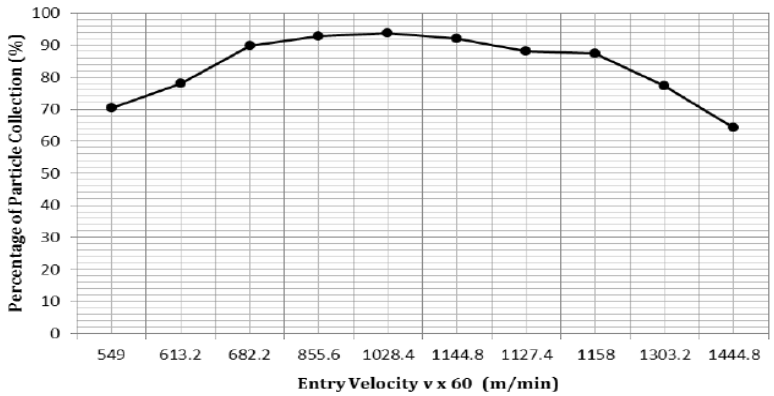

Figure 10: Entry Velocity versus Percentage of Particle collection.

The figures 9 and 10 show the effects of Pressure drop and Entry velocity on percentage fine particle collection in the Cyclone. The percentage fine particle collection increases as pressure drop increases and seems slightly stable between 22.64 and 33.65 N/m2 before decreasing to 85.66 N/m2. A similar trend is also seen as percentage fine particle collection

increases as Entry velocity increases and seems slightly stable between 682.2 and 1158 x 60 m/min before decreasing to 1444.8 x 60 m/min. it can also be inferred that optimum fine particle collection (Above 88%) can be achieved at a range of 22.64 to 54.8 N/m2 and 682.2 to 1158 x 60 m/min of pressure drops and Entry velocities respectively.

IV. CONCLUSION

Inlet velocity obtained for selected speeds was between 12.23m/s and 28.95m/s at no-load basis while it was 9.15m/s and 24.08m/s when samples were introduced into the system. The graphs plotted for velocity and pressure profiles on no-load and load basis were both represented by third order polynomial functions of differing coefficients and constants. Similar trend was noticed for pressure drop along the cyclone with values between 35.44 N/m2 and 119.64 N/m2 at no-load basis while at load basis it was between 30.86 N/m2 and 85.66 N/m2. Also optimum fine particle collection (Above 88%) can be achieved at a range of 22.64 to 54.8 N/m2 and 682.2 to 1158 x 60 m/min of pressure drops and Entry velocities respectively.

REFERENCES

1. Baker, R.V., Hughes S.E., Gillum M.N and Green J.K. “Improvements for cotton gin trash cyclones”. Trans. ASAE, 1997; 40(1): 5–12.
2. Baker, R.V. and Hughs S.E. (1998) “Modifications for 1D3D cyclones”: p. 1666–1670. In Proc. Beltwide Cotton Conf., San Diego, CA. 5-9 Jan. 1998. Natl. Cotton Council; Am., Memphis, TN.
3. Baker, R.V. and Hughs S.E. “Influence of air inlet and outlet design and trash exit size on 1D3D cyclone performance”. Trans. ASAE, 1999; 42(1): 17–21.
4. Barber, E.M., Zhang Y. and Sokhansanj S. “A transient calorimetry method used to estimate the ventilation rate in an enclosed airspace”. ASAE Paper No. NCR, 1988; 88-603. St. Joseph, MI: ASABE
5. Cortés, C. and Gil A., “Modeling the gas and particle flow inside cyclone separators”: Progress in Energy and Combustion Science, 2007; 33: 409–452.
6. David Heeley. (2005) Understanding Pressure and Pressure Measurement: Free scale Semiconductor, Application Note. Phoenix, Arizona AN1573.
7. Dennis, R and Klemm H.A. (1979). Fabric Filter Model Change: Vol. 1, Detailed Technical Report, EPA -600/7-79-043a, NTIS PB 293551.

8. De Otte R.E., A Model for the Prediction of the Collection Efficiency Characteristics of a Small, Cylindrical Aerosol Sampling Cyclone: J. Aerosol Sci. Technol., 1990; 12: 1055-1066.
9. [EPA] Environmental Protection Agency: APTI 413, Cyclones; Control of Particulate Matter Emissions: Student Manual. Newport News, Virginia. Pp 1-5 (accessed 2011).
10. Faulkner W. B., Shaw, B. W. "Efficiency and Pressure Drop of Cyclones across A Range of Inlet Velocities" Applied Engineering in Agriculture; ASABE, 2005; 22(1): 155-161.
11. Faulkner, W.B., Buser M.D., Whitelock D.P. and Shaw B.W. "Effects of cyclone diameter on performance of 1D3D cyclones: collection efficiency". Trans. ASABE, 2007; 50(3): 1053–1059.
12. Faulkner, W.B., Buser M.D., Whitelock D.P. and. Shaw B.W. "Effects of cyclone diameter on performance of 1D3D cyclones: cut-point and slope". Trans. ASABE 2008; 51(1): 287–292.
13. Funk, P.A., Hughs S.E. and Holt G.A. (2001) "Dust cyclone design". Appl. Eng. Agric., 2001; 17(4): 441–444.
14. Holt, G.A., Baker R.V and Hughs S.E. "Evaluation of static pressure drops and PM10 and TSP emissions for modified 1D-3D cyclones". Trans. ASABE, 1999; 42(6): 1541–1547.
15. Hu, L.Y., Zhou L.X., Zhang J. and Shi M.X. "Studies on strongly swirling flows in the full space of a volute cyclone separator". AIChE Journal, 2005; 51(3): 740–749.
16. Lim K. S., Kwon S. B., and. Lee K. W, Characteristics of the Collection Efficiency for A Double Inlet Cyclone with Clean Air: [J]. Aerosol Sci., 2003; 34: 1085-1095.
17. Lim, K.S., Kim H.S. and Lee K.W. Characteristics of the collection efficiency for a cyclone with different vortex finder shapes. Aerosol Sci. 2004; 35: 743–754.
18. Obermair, S. and Staudinger G. "The dust outlet of a gas cyclone and its effects on separation efficiency". Chem. Eng. Technol, 2001; 24(12): 1259–1263.
19. Obermair, S., Gutschi C., Woisetschlager J. and Staudinger G. "Flow pattern and agglomeration in the dust outlet of a gas cyclone investigated by phase Doppler anemometry" Powder Tech., 2005; 156: 34–42.
20. Ogawa, A. and Arakawa M. Control of collection efficiency for axial flow cyclone dust collectors with fixed guide vanes and with funnel shaped exit pipes. J. Thermal Sci., 2006; 15(3): 240–250
21. Oriaku, E.C, Edeh, J.C, Nwannewuihe, H.U and Onwukwe, M. (2011). Official work Docunment: Projects Development Institute (PRODA) Enugu, Nigeria.

22. Peng, W., Hoffman A.C., Boot P.J.A.J, Udding A., Dries H.W.A, Ekker A. and Kater J. "Flow pattern in reverse-fow centrifugal separators". Powder Tech., 2002; 127: 212–222.
23. Peng, W., Hoffman A.C., Dries H.W.A, Regelink M.A. and Stein L.E. "Experimental study of the vortex end in centrifugal separators: the nature of the vortex end". Chem. Eng. Sci., 2005; 60: 6919–6928.
24. Shepherd, C. B. and Lapple, C.E. Flow pattern and pressure drop in cyclone dust collectors: Ind. Eng. Chem., 1940; 32(9).
25. Schnelle, B. K and Brown, A.C. Air pollution Control Technology Handbook: Chapter 21, CRC Press LLC; 2002; 311-321.
26. Stairmand, C. J., The design and performance of cyclone separator: Trans. Ind. Chem. Eng., 1951; 29: 356-383.
27. Whitelock, D.P. and. Buser M.D. "Multiple series cyclones for high particulate matter concentrations". Appl. Eng. Agric., 2007; 23(2): 131-136. www.idahopacific.com/index.html. Accessed September 2010.
28. Wikipedia (2010) http://en.wikipedia.org/wiki/Flour accessed March, 2010.
29. Wikipedia (2010) http://en.wikipedia.org/wiki/Mass_fraction_%28chemistry%29 accessed 2012.
30. Xiang, R., Park S.H. and Lee K.W. "Effects of cone dimension on cyclone performance". J. Aerosol Sci., 2001; 32: 549–561.